Impact of Power Control on Performance of IEEE 802.11 Wireless Networks

Ivan Wang-Hei Ho, *Student Member*, *IEEE* and Soung Chang Liew, *Senior Member*, *IEEE*

Abstract — *Optimizing spectral reuse is a major issue in large-scale IEEE 802.11 wireless networks. Power control is an effective means for doing so. Much previous work simply assumes that each transmitter should use the minimum transmit power needed to reach its receiver, and that this would maximize the network capacity by increasing spectral reuse. It turns out that this is not necessarily the case, primarily because of hidden nodes. This paper shows that in a network with power control, avoiding hidden nodes can achieve higher overall network capacity compared with the minimum-transmit-power approach. It is not always best to use the minimum transmit powers even from the network capacity viewpoint. Specifically, we propose and investigate two distributed adaptive power control algorithms that minimize mutual interferences among links while avoiding hidden nodes. Different power control schemes have different numbers of exposed nodes and hidden nodes, which in turn result in different network capacities and fairness. Although there is usually a fundamental tradeoff between network capacity and fairness, we show that, interestingly, this is not always the case. In addition, our power control algorithms can operate at desirable network- capacity-fairness tradeoff points, and can boost the capacity of ordinary non-power-controlled 802.11 networks by two times while eliminating hidden nodes.*

Keywords — Wireless Networks, WLAN, Power Control, 802.11, Network Capacity, Scalability, CSMA/CA, Ad-hoc Networks, Hidden Nodes, Exposed Nodes.

I. INTRODUCTION

Optimizing spectral reuse is a major issue in large-scale IEEE 802.11 wireless networks. Power control is an effective means for doing so, and can allow 802.11 and 802.11-like wireless networks to achieve scalable capacity [1]. Much of the previous work on power control focuses on maximizing spectral reuse by minimizing the transmit powers of nodes [2] [3] [4]. However, such power control algorithms may not be desirable in that they overlook the effect of hidden nodes (HN), which may give rise to unfair network bandwidth distributions and bandwidth oscillations [5] [6].

HN can be eliminated by extending the carrier-sensing range [5]. However, doing so may cause the exposed-node (EN) problem in which links that do not otherwise interfere with each other are not allowed to transmit simultaneously because of carrier sensing, resulting in low spectral reuse.

This paper proposes and investigates two distributed adaptive power control algorithms that can avoid HN. In particular, in these algorithms the transmit powers of transmitters are adapted to the positions of their surrounding links besides the connectivity requirements with their receivers. These algorithms make sure that (i) links that do not mutually interfere with each other remain non-interfering, and that existing interfering links may become non-interfering after power adjustments; and (ii) HN will not be created. In general, these two algorithms can boost the total throughput in ordinary non-power-controlled 802.11 networks by more than two times while preserving fairness in the network. Moreover, one of them can simultaneously achieve better fairness and network capacity in the network when compared with the minimum-transmit-power approach. The second contribution of this paper is as follows. In a *non-power-controlled network*, there is generally a tradeoff between HN and EN, which translates to a tradeoff between fairness and overall network capacity. Interestingly, we show in this paper that for *power-controlled networks*, this is not always the case. Indeed, if we allow too many HNs in the network, even if ENs are reduced, both network capacity and fairness can deteriorate simultaneously.

This work was supported by the Competitive Earmarked Research Grant (Project Number 414305) established under the University Grant Committee of the Hong Kong Special Administrative Region, China.

Ivan W. H. Ho was with the Department of Information Engineering, the Chinese University of Hong Kong. He is now with the Department of Electrical and Electronic Engineering, Imperial College London, U.K. (email: wh.ho@imperial.ac.uk)

S. C. Liew is with the Department of Information Engineering, the Chinese University of Hong Kong, Hong Kong. (email: soung@ie.cuhk.edu.hk)

Related Work

The current commercial 802.11 products do not have the feature of power control, and this is a major reason why current 802.11 wireless networks are not scalable [9]. Given the confine of a fixed geographical area, installing more access points (APs) do not boost the overall capacity beyond certain limit. A motivation of this work is to explore how power control can be used to scale 802.11 networks. Reference [9] considers a scheme to scale 802.11 networks which requires substantial change of the underlying MAC protocol. In contrast, this paper focuses on dynamic adjustment of transmission power to scale the network. We also note that most current 802.11 products do not give accurate measured power values through their standard user interface. The algorithms in this paper require more accurate power measurement schemes. Although 802.11 networks are in its early stage of deployment, it is already enjoying exponential growth throughout the world. As more and more 802.11 networks are being installed in the same area, they will mutually interfere with each other, and the capacity of each network will be reduced substantially. The current cellular telephony network already makes use of power control to scale capacity. We believe the introduction of power control in future 802.11 wireless networks will become essential if their deployment continues unabated.

To provide the context of our work, Figure 1 shows a possible classification of various approaches for power control. Most previous investigations adopt the minimum-transmit-power approach (e.g., [2] and [3]). The COMPOW protocol in [2] selects a *common* minimum transmit power for all nodes such that network connectivity is preserved. Essentially, the transmit powers of all nodes are set to maximum of the minimum power requirements of all links. The CLUSTERPOW protocol [2], on the other hand, transmit powers of nodes may vary, and each node forwards packets using the smallest powers required to reach their destinations. Reference [3] is similar in that it proposed a distributed power-control algorithm that allows nodes to learn the minimum transmit powers required to successfully transmit to nearby nodes. The learning is done through RTS/CTS.

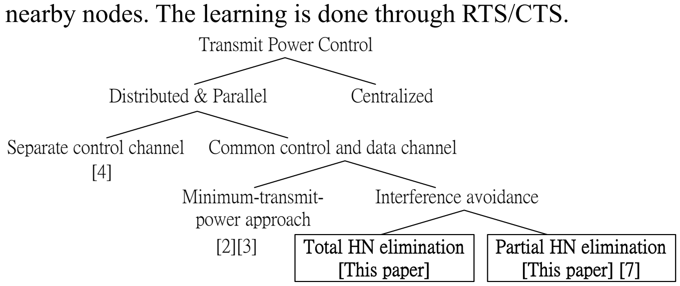

Figure 1. Classification of related work on transmit power control.

In contrast to [2], [3], and our work here, [4] proposed a Power Controlled Multiple Access (PCMA) protocol that uses a separate control channel for "busy tone" instead of RTS/CTS to avoid collisions, in which the signal strength of the busy tones received by a node is used to determine the power level at which this node may transmit without interfering with other on-going transmission.

Reference [7], as in our work here, does not assume the use of minimum transmit powers. It proposed to always transmit RTS/CTS and intermittently transmit data packets at maximum power. The increased interference and EN effects due to the use of large transmit power are ignored. The approach aims to save energy, but spectral reuse is not improved.

Instead of just using minimum transmit powers, this paper proposes to adjust the transmit power of a transmitter based on its connectivity requirement with its receiver as well as potential interferences with its surrounding links. Intuitively, if the transmit power of a transmitter is decreased, it is more likely for other nodes to interfere with its receiver because of the decreased SIR; on the flip side, the interference of the transmitter to other nodes will be reduced. How to judiciously adjust the powers of neighboring nodes based on the distances among them (more exactly, the power-transfer matrix that describes their power relationships) in a distributed and parallel manner is our key focus here. As described earlier, there is generally a tradeoff between EN and HN. The two algorithms proposed in this paper aim to eliminate HN in the network. The algorithms, however, are actually amenable to modifications that aim to decrease EN at the cost of some HN. The tradeoff between EN and HN (hence, network capacity and fairness) are explored. Based on such modifications, in the later part of this paper, we find that it is not always true that we can improve network capacity by sacrificing fairness, and vice versa. Indeed, both network capacity and fairness can deteriorate simultaneously when there are too many HNs in the network, even though ENs have been decreased.

The rest of this paper is organized as follows. Section II defines graph models that capture the interference relationships among links to facilitate algorithmic designs. Section III presents our first power control algorithm called *Decoupled Adaptive Power Control (DAPC)*, in which each node only monitors its local surrounding to effect its own power adjustment. Different nodes can compute and adjust their transmit powers simultaneously while making sure that no new interference relationships and HN will be created in the process. Section IV presents our second power control algorithm called *Progressive-Uniformly-Scaled Power Control (PUSPC)*, which performs better than DAPC by solving a deadlock problem from which DAPC may suffer. The combination of DAPC followed by PUSPC is also investigated. Section V evaluates the performance of our proposed algorithms based on the criteria of network capacity, fairness, and amounts of EN and HN, and demonstrated the influence of the tradeoff between EN and HN on network capacity. Finally, Section VI concludes this paper.

II. GRAPH MODELS FOR CAPTURING TRANSMISSIONS CONSTRAINTS AND HIDDEN-NODE PROBLEMS

This section presents graph models for capturing simultaneous-transmissions constraints and HN to facilitate algorithmic design. Links in the network are mapped to vertexes, and links that interfere or interact with each other are related through edges in the graph.

Subsection A provides an example to illustrate the shortcomings of power control with minimum transmit powers. Subsections B, C, and D present the components in our graph models. Specifically, Subsection B considers the physical-collision constraints due to the receiver's inability to decode its signal when the powers received from other transmitting sources are large (i.e., small SIR). They form the basis of a link-interference graph. Subsection C considers the protocol-collision-prevention constraints imposed by carrier sensing of 802.11 against simultaneous transmissions. They form the basis of a protocol-collision-prevention graph. Subsection D defines the "ideal" carrier-sensing operation. They form the basis of an ideal protocol-collision-prevention graph. Subsection E defines HN and EN in a formal manner in terms of the differences between the *802.11 protocol-collision-prevention graph* in Subsection C and the *ideal protocol-collision-prevention graph* in Subsection D. Finally, Subsection F introduces a metric for performance evaluation purposes.

A. An Example Illustrating Shortcomings of Minimum-Transmit-Power Approach

We assume the following power-transfer relationship: $P(a,b) = k \cdot P_a / r^{\alpha}$, where $P(a, b)$ is the power received by node b from node a; P_a is the transmit power of node a; r is distance between the two nodes; $\alpha > 2$ is the path-loss exponent; and k is a constant. Note that this expression is only for analysis purpose. In the running of our algorithms, the power-transfer relationships are obtained through power measurements. Thus, power information instead of distance information is used in our algorithms. Let T_i and R_i denote the transmitter and receiver of link i. For brevity, we also use T_i and R_i to denote their positions. So, $| a - b |$ denotes the distance between nodes a and b. We also assume that the SIR requirement, K, is such that if $KP(T_2, R_1) > P(T_1, R_1)$, then T_2 will interfere with the reception at R_1.

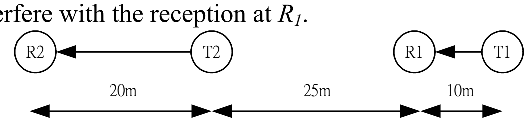

Figure 2. An example to illustrate the shortcomings of minimum-transmit-power approach.

Consider links 1 and 2 in Figure 2, and assume basic-mode access with no RTS/CTS. The default parameter values used in NS-2 [8] are K=10, k=5, α=4, $TxRange$ = 250m, $PCSRange$ = 2.186*$TxRange$ = 550m, Rx_{th}=3.652e-10W, where $PCSRange$ and $TxRange$ are respectively the physical carrier-sensing range and transmission range, Rx_{th} is the minimum received power needed for signal detection. The corresponding transmit power given the above $TxRange$ and Rx_{th} is 0.281W.

By plugging in the above NS-2 parameter values, we find that $KP(T_2, R_1) < P(T_1, R_1)$, but $KP(R_1, T_2) > P(R_2, T_2)$ according to the locations of links 1 and 2. This means that the ACK of R_1 can interfere with the reception of ACK from R_2 to T_2. However, since both T_2 and R_1 are within the $PCSRange$ = 550m, the potential collision can be prevented by physical carrier sensing.

Suppose now we adjust the transmit powers of the four nodes to their minimum. After the adjustment, $P(T_1, R_1) = P(R_1, T_1) = P(T_2, R_2) = P(R_2, T_2) = Rx_{th}$, and the $TxRanges$ of link 1 and link 2 become 10m and 20m respectively. Now, $KP(R_1, T_2)$ = 9.3e-11 < $Rx_{th} = P(R_2, T_2)$, but $KP(T_2, R_1)$ = 1.5e-9 > $Rx_{th} = P(T_1, R_1)$. Thus, the DATA packets of T_2 can interfere with the reception of DATA from T_1 to R_1 now. Moreover, $PCSRange$ of T_1 = 2.186 x 10 = 21.86 < $|T_2 - T_1|$ after power control. This means link 1 cannot forewarn link 2 when link 1 transmits. So, we see that the use of minimum transmit powers creates the possibility of DATA-DATA collisions. Furthermore, these collisions cannot be prevented by carrier sensing, causing the classical HN phenomenon. The use of minimum transmit powers are highly undesirable in this case.

We could also find examples in which HN is eliminated by using minimum-transmit power. However, according to our simulation results, more HN instances are created than eliminated by the minimum-transmit power approach. For example, in a randomly generated ad-hoc topology with 100 links in a domain of 1x1 km^2, there are originally 106 HN instances; but the number of HN instances increases to 542 after adopted the minimum-transmit-power approach. The reader is referred to Part E for our definition and measurement of HN in the network.

The above example points out that one must consider not just the power requirement of a link in terms of its SNR (i.e., the minimum power required at the receiver Rx_{th} so that the signal is sufficiently above the noise floor), but its SIR with respect to the potential interferences with the surrounding links. That is the basis on which the power control algorithms in this paper are designed. To aid our algorithm designs, the next few subsections describe graph models for capturing the relationships among links within vicinity of each other.

B. Link-Interference Graph from Physical-Collision Constraints

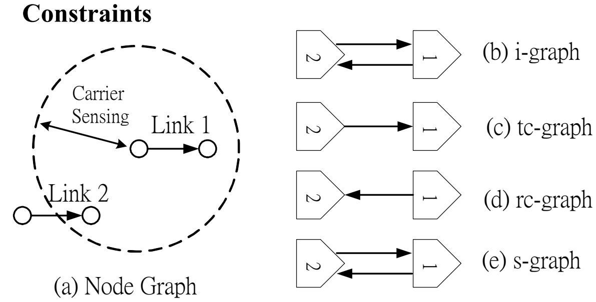

Figure 3. Mapping of a network topology a) to b) i-graph, c) tc-graph, d) rc-graph and e) s-graph.

A *Link-Interference Graph (i-graph)* can be used to represent the physical-collision constraints graphically. It basically captures the effects of SIR among links. Consider the simple network topology in Figure 3a. As illustrated in Figure 3b, in an i-graph, an arrow-shape vertex represents a wireless link with the arrowhead pointing toward the receiver.

In the example of Figure 3b, there is a directional i-edge from vertex 1 to vertex 2, and vice versa, because the transmitter of link 1 and receiver of link 2 are so close to each other that they interfere with the reception at each other. DATA of T_1 may collide with DATA of T_2 at R_2; and ACK of R_2 may collide with ACK of R_1 at T_1. Although not the case in Figure 3, in general it is possible that there is an i-edge from link 2 to link 1 but not the other way round direction due to the differences in link length and powers used. More formally, there is an i-edge from vertex 2 to vertex 1 if any of the (1) – (4) is satisfied.

$$P_{T1}|T_2 - R_1|^{\alpha} < KP_{T2}|T_1 - R_1|^{\alpha} \quad (1)$$

$$P_{R1}|T_2 - T_1|^{\alpha} < KP_{T2}|T_1 - R_1|^{\alpha} \quad (2)$$

$$P_{T1}|R_2 - R_1|^{\alpha} < KP_{R2}|T_1 - R_1|^{\alpha} \quad (3)$$

$$P_{R1}|R_2 - T_1|^{\alpha} < KP_{R2}|T_1 - R_1|^{\alpha} \quad (4)$$

For (1), the power received by R_1 from T_1 must be sufficiently larger than the power received by R_1 from T_2 in order that the signal from T_1 can be successfully decoded. Let the Signal-to-Interference requirement be K (e.g., 10dB). Then, collision occurs when $P(T_1, R_1) < K\,P(T_2, R_1)$. Plugging in the power-transfer relationship $P(a, b) = kP_a / | a - b |^{\alpha}$ gives (1). (2) – (4) can be derived similarly by considering different combinations of nodes in links 1 and 2.

Constraints (1) – (4) correspond to DATA-DATA collision, DATA-ACK collision, ACK-DATA collision and ACK-ACK collision, from link 2 to link 1, respectively. Similarly, link 1 can also interfere with link 2 with four similar constraints by interchanging the indexes 1 and 2 in (1) – (4).

Note in this paper that we model links as directional links. So, bidirectional links between two nodes will be considered as two links. For example, if link 1' is the reverse-directional link of link 1, then $T_{1'} = R_1$ and $R_{1'} = T_1$ in our model, and the links will be modeled separately as vertexes 1 and 1' in our graph model.

C. Protocol-Collision-Prevention Graphs

We next consider the effect of 802.11 carrier sensing. The goal of carrier sensing is to prevent simultaneous transmissions that will collide. Two protocol-collision-prevention graphs can be used to model the carrier sensing: the tc-graph models the effect of carrier sensing by transmitters, and the rc-graph models that by receivers.

In the tc-graph, there is a directional tc-edge from vertex 1 to vertex 2 if T_2 can sense the transmission on link 1 so that if T_1 is already transmitting its DATA, T_2 will not transmit. Formally, there is a tc-edge from vertex 1 to vertex 2 if any of the inequalities (5) – (7) is true.

$$|T_2 - T_1| < VCSRange(P_{T1}) \qquad \textbf{(5)}$$

$$|T_2 - R_1| < VCSRange(P_{R1}) \qquad \textbf{(6)}$$

$$|T_2 - T_1| < PCSRange(P_{T1}) \qquad \textbf{(7)}$$

where $VCSRange(P_a)$ is the virtual carrier-sensing range due to the transmissions of RTS/CTS by node a with transmit power P_a ; and $PCSRange(P_a)$ is the physical carrier-sensing range due to the DATA transmission by node a.

In the example of Figure 3c, we assume T_1 and T_2 are sufficiently far apart that they cannot physically sense each other. However, the T_1 can sense the CTS of R_2, but T_2 is so far away from T_1 and R_1 that it cannot sense the RTS and CTS from them. So, there is a tc-edge from link 2 to link 1 but not the other way round.

In the rc-graph, there is a directional rc-edge from vertex 1 to vertex 2 if the R_2 can sense the transmission on link 1. Specifically, there is an rc-edge from link 1 to link 2 if any of the inequalities (8) – (10) is satisfied.

$$|R_2 - T_1| < VCSRange(P_{T1}) \qquad \textbf{(8)}$$

$$|R_2 - R_1| < VCSRange(P_{R1}) \qquad \textbf{(9)}$$

$$|R_2 - T_1| < PCSRange(P_{T1}) \qquad \textbf{(10)}$$

In the default mode of 802.11 in commercial products and NS-2, when T_1 is already transmitting, T_2 can still transmit if there is an rc-edge, but no tc-edge, from vertex 1 to vertex 2. However, R_2 will ignore the DATA (RTS) frame and not return an ACK (CTS). The rationale for R_2 not returning an ACK (or CTS) to T_2 is that the ACK (CTS) may interfere with the ongoing transmission on link 1.

In the example of Figure 3d, there is an rc-edge from link 1 to link 2 but not in the other direction since R_2 can sense the RTS of T_1, but R_1 is so far away from link 2 that it cannot sense any RTS/CTS from it.

D. Ideal Protocol-Collision-Prevention Graph

The previous subsection was about the tc-graph and rc-graph that correspond to the actual carrier-sensing operation of 802.11. However, 802.11 carrier sensing may not be ideal in that it may (i) prevent non-collision-causing simultaneous transmissions, and (ii) fail to prevent collision-causing simultaneous transmissions. We introduce the concept of a s-graph with *s-edges* (*should-forewarn edges*) to describe the *ideal* carrier-sensing operation. The comparison of s-graph, tc-graph, and rc-graph allows us to define HN and EN in a formal manner, which aids our algorithmic design later.

In an s-graph, there is an s-edge from vertex 1 to vertex 2 if link 1 should forewarn link 2 when it transmits, due to the presence of an i-edge from 1 to 2, or an i-edge from 2 to 1. Equivalently, there are two s-edges, one from 1 to 2, and one from 2 to 1, if there is an i-edge from vertex 1 to vertex 2. The definition of s-edge is as such because no matter link 1 or link 2 transmits first, transmission at link 2 will fail. Therefore, when link 2 transmits, it should first forewarn link 1 not to transmit. Similarly, when link 1 transmits, it should forewarn link 2 not to transmit. In short, s-edges always exist in pairs.

In the example of Figure 3e, there are two s-edges between links 1 and 2, one in each direction. It turns out that there are also two i-edges in this example. However, even if there were only one i-edge between links 1 and 2, we would still have the two s-edges in both directions.

E. Definition of HN and EN and their Investigation using Graph Model

Figure 4 shows the Venn Diagram depicting the relationships among different types of edges and the inequalities that define them. In the Venn Diagram, the set elements are link duples (i, j). Each link duple (i, j) represents the relationship from vertex i to vertex j. It could be a tc-edge, rc-edge, s-edge, none of them, or a combination of them.

We now provide formal definitions for HN and EN. Based on the definition, we introduce the metric to measure the severity of HN and EN in the network, which will be used in this paper to analyze our simulation results. Strictly speaking, the HN and EN phenomena are due to relationships between links rather than between nodes. However, we will continue to use these terms since they are already commonly used.

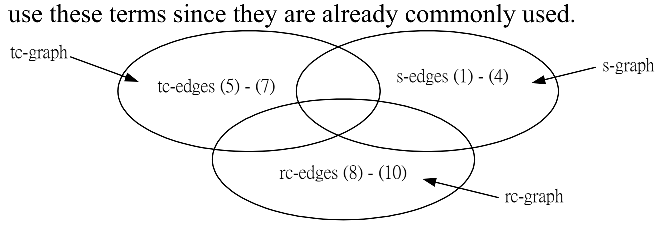

Figure 4. Relationships among s-edges, tc-edges and rc-edges in s-graph, tc-graph and rc-graph; and the constraints associated with the edges.

Definition of HN: There is HN from link i to link j if (i, j) is not a tc-edge, but is an s-edge or rc-edge. Link i is said to be hidden from link j in this case.

Definition of EN: There is EN from link i to link j if (i, j) is not an s-edge, but is a tc-edge or rc-edge. Link j is said to be exposed to link i in this case.

With respect to the above HN definition, simultaneous transmissions on links i and j cannot both be successful.

However, link j cannot be prevented from transmitting when link i is already transmitting. As for the EN definition, there is actually no physical interference between links i and j in terms of their SIRs. However, the existence of a tc-edge from i to j will prevent j from transmitting when i is already transmitting; while the existence of an rc-edge will prevent the success of the transmission by link j because R_j will not reply to T_j. Thus, HN is a phenomenon whereby colliding transmissions fail to be prevented by carrier sensing, while EN is a phenomenon non-colliding transmissions or their success are prevented by carrier sensing. They are both caused by the discrepancies among s-edges, tc-edges and rc-edges.

Let us denote the set of s-edges by S, the set of tc-edges by TC, and the set of rc-edges by RC. As measures of the severity of HN and EN in the overall network, we can look at

# of HN-causing edges: $N_{HN} = |S \cup RC| - |TC \cap (S \cup RC)|$

# of EN-causing edges: $N_{EN} = |TC \cup RC| - |(TC \cup RC) \cap S|$

For the network to be HN-free, we require $TC = S \cup RC$ so that $N_{HN} = 0$. For the network to be EN-free, we require $S = TC \cup RC$ so that $N_{EN} = 0$. In general, 802.11 networks cannot be both HN-free and EN-free. We may define normalized Miss Ratio = $N_{HN} / |S \cup RC|$ and False-alarm Ratio = $N_{EN} / |S \cup RC|$ to measure the severities of HN and EN in a given network. The reason for using the normalization factor $|S \cup RC|$ is that it corresponds to the number of cases where simultaneous transmissions are not allowed, or will not be successful.

In the simulations of our proposed power control algorithms in Section V, the network has no HN initially when our power-control algorithms start running, and the algorithms are required to maintain the HN-free property throughout their execution. Generally speaking, to maintain the HN-free property, (i) the carrier-sensing range must be sufficiently large and (ii) a so-called receiver restart (RS) mode must be effected (the reader is referred to [5] for details). As far as our work here is concerned, the RS mode is assumed and we simulate the network in basic mode with the initial physical carrier-sensing range, *PCSRange* set to 3.78 *TxRange*, the maximum transmission range of DATA at the initial transmit power.

F. Attacking Cases

This subsection introduces another performance metric, *number of attacking cases*, which corresponds to the number of cases where simultaneous transmissions are either *not* allowed, or where allowed, will not be successful. Link i is said to be attacking link j if (i, j) is an i-edge, a tc-edge, or a rc-edge.

The number of attacking cases in a network is the sum of the number of attacking cases from link i to link j over all i and j. Specifically, for all (i, j), $i \neq j$:

If (i, j) is an i-edge, then add 2 to # attacking cases;
else if (i, j) is a tc-edge, then add 1 to # attacking cases;
else if (i, j) is an rc-edge, then add 1 to # attacking cases.

The above enumeration process takes into account the order of transmissions. If (i, j) is an i-edge, it does not matter whether i or j transmits first, signal at j will be corrupted. So, there are two cases where i can "attack" j. On the other hand, if (i, j) is a tc- or rc-edge, transmission at link j will not be allowed or will fail only if link i transmits first. So, there is only one case. If there are L directional links, then the above summation will be over $L(L - 1)$ link pairs.

III. DECOUPLED ADAPTIVE POWER CONTROL (DAPC)

This section presents our first distributed adaptive power control algorithm, *Decoupled Adaptive Power Control (DAPC)*. The main essence of DAPC is to decouple the power adjustments of individual links to the extent that is possible, so that many links can adjust their powers simultaneously in a distributed and parallel manner. In DAPC, (i) a node only needs to gather information from nearby nodes that are within a certain "radius" to it; and (ii) powers used by links that are far apart can be adjusted simultaneously. Each individual node will perform its power adjustments based on its own computation through a number of iterations. In Subsection A, we first discuss how much power can be reduced by a link in each iteration in our algorithm. Subsection B provides a Power Exchange Algorithm (PE) [9] for links to gather power information and discuss how the "radius" in (i) can be bounded with the concept of *Interaction Range* (*IntRange*). Based on the principles in Subsections A and B, Subsection C discusses the implementation of DAPC, which guarantees that no new i-edges or HN will be created in each iteration. Subsection D points out, however, that DAPC may face a deadlock problem that limits its performance. Deadlock-free power control will be presented in Section IV.

A. Per-iteration Power Adjustment

In this algorithm, when individual links perform power reduction in each iteration, they assume the transmit powers of its surrounding links remain unchanged. When reducing its power, a link must make sure that 1) the connectivity between its transmitter and receiver can be maintained; 2) the power reduction does not create new i-edges from other links to itself, even if other links do not reduce their powers; and 3) the carrier-sensing range with the reduced power is still sufficient to cover interfering nodes, such that no new hidden nodes are created. Note that if all links perform 2), no new i-edges will be created in the network because each link assumes the worst-case SIR in its power adjustment. The steps are elaborated below for an arbitrary link labeled as link 1.

1. **Ensuring reduced power satisfies minimum received power threshold to maintain link connectivity:** To guarantee connectivity from T_1 to R_1, the minimum transmit power of T_1 must be bounded below by

$$P_{\min}(T_1) = \frac{Rx_{th}}{G(T_1, R_1)} = \frac{P_{T1}}{P(T_1, R_1)} \times Rx_{th} \quad \textbf{(11)}$$

where Rx_{th} is the minimum necessary received signal strength, and $G(i, j) = P(i, j)/P_i$ is the power-gain function from node i to node j that can be computed from the current transmit power P_i used by node i and the current power of node i received by node j, $P(i, j)$. Similarly, the minimum transmit power of R_1 must be bounded below by

$$P_{\min}(R_1) = \frac{Rx_{th}}{G(R_1, T_1)} = \frac{P_{R1}}{P(R_1, T_1)} \times Rx_{th} \quad \textbf{(12)}$$

$G(T_1, R_1) = G(R_1, T_1)$ can be found from the Power Exchange Algorithm in Subsection B.

2. **Ensuring reduced power does not create new i-edges:** To ensure that *no new i-edges to vertex 1 will be created when T_1 and R_1 reduce their transmit powers*, we need to consider the interferences from surrounding links. Let N_{T1} and N_{R1} be respectively the sets of nearby transmitting and receiving nodes that are not currently interfering with T_1 and R_1, but which may potentially do so if the powers of T_1 and R_1 are reduced too aggressive. As a conservative measure, we assume the powers of the nodes in N_{R1} and N_{T1} are not changed when computing the acceptable new powers of T_1 and R_1. We require

$$P_{adjusted}(T_1) \geq KP(n, R_1)/G(T_1, R_1) \quad \forall n \in N_{R1} \qquad \textbf{(13)}$$

$$P_{adjusted}(R_1) \geq KP(n, T_1)/G(T_1, R_1) \quad \forall n \in N_{T1} \qquad \textbf{(14)}$$

Note that (13) is to ensure there is sufficient SIR at R_1 for the DATA on link 1, and (14) is to ensure there is sufficient SIR at T_1 for the ACK on link 1. In general, N_{T1} and N_{R1} do not need to cover all nodes in the network. Only nodes n that satisfy the following need to be considered:

(i) $n \in N_{T1}$ if and only if $P(n, T_1) \geq Rx_{th} / K$

(ii) $n \in N_{R1}$ if and only if $P(n, R_1) \geq Rx_{th} / K$

3. **Ensuring *PCSRange* of reduced power is enough to cover interfering nodes:** In this paper, we focus on basic-mode access. This requirement is to ensure that the physical carrier sensing in 802.11 continues to avoid HN after each power adjustment. Let M_{T1} denote the set of transmitters whose link has a s-edge to link 1 and vice versa. This means that $\forall\, m \in M_{T1}$, the *PCSRange* of T_1 must be able to reach m. Note that the difference between M_{T1} and N_{T1} is that the former refers to nodes whose links already have interference relationships with the link 1, whereas the latter refers to nodes that do not currently interfere with T_1 but may do so if power adjustment is not done right. Before T_1 transmits, it must be able to warn the nodes in M_{T1} not to transmit through physical carrier sensing. Therefore, to maintain the HN-free property, the following inequality must be satisfied:

$$P_{adjusted}(T_1) \geq Rx_{th}^{PCS} / G(T_1, m) \quad \forall m \in M_{T1} \qquad \textbf{(15)}$$

where Rx_{th}^{PCS} is the receiver sensitivity threshold for PHY header, which is generally smaller than Rx_{th} so that *PCSRange* is larger than *TxRange*. For example, if PHY are transmitted at $1/r_{PCS}$ the rate of DATA, as an approximation, we may set $Rx_{th}^{PCS} = Rx_{th} / r_{PCS}$. Note that we have assumed the same transmit power is used to carry DATA/ACK and PHY on a link.

Steps 1, 2, and 3 are combined as follows. We set $P_{adjusted}(T_1)$ to the maximum of (11), (13) and (15). Then, we set $P_{adjusted}(R_1)$ to the maximum of (12) and (14). Note that in DAPC, the transmitter and receiver of a link may use different power levels.

The nodes in N_{T1}, N_{R1}, and M_{T1} in steps 2 and 3 define an *Interaction Range* (*IntRange*) over which other links can interfere with or can potentially interfere with link 1. Specifically, faraway nodes outside of *IntRange* not belonging to N_{T1}, N_{R1}, and M_{T1} need not be considered by link 1 when it adjusts the transmit powers used by its transmitter for DATA and its receiver for ACK. Note that not all links within *IntRange* can interfere with link 1, but all links outside *IntRange* are guaranteed not to do so.

B. Power Exchange Algorithm

In [9], a Power Exchange Algorithm (PE) was proposed for establishing the i-graph of a network. Our power adjustment procedure in Subsection A requires not only the knowledge of the current i-edges, but also the power-transfer relationships between nearby nodes so that we can ensure that no new i-edges will be created and the *PCSRange* is sufficient after power adjustment. We extend the PE in [9] for our purpose here.

Power-Exchange packets (PE packets) are special packets periodically broadcasted by nodes to exchange power information with neighbors. We assume the transmit powers of these packets are the same as the transmit powers of regular packets like DATA/ACK/RTS/CTS.

Consider an arbitrary node a. The PE packets sent by node a contain three types of information: (i) Active links (a, b) or (b, a), where b is any other node which forms an active link with a; (ii) Transmit power P_a of node a; (If node a is an AP, we assume it uses different P_a for different client stations and establishes multiple links with clients) (iii) "Power set", as described below. The identity of the node a is implicit in the MAC address of its PE packets.

- Node a monitors the power it receives from other nodes and keep this information in a power set $PS_a = \{[b, P(b, a)], [c, P(c, a)], \ldots\}$.
- Node a periodically broadcasts a PE packet at a rate lower than the data rate to increase the transmission range.
- Node a gathers information from the PE packets received from its neighbors by measuring the powers of the received PE packets as well as looking into their contents.

Condition for Correct Operation of PE: Interaction Range

The following conditions are sufficient to ensure that the necessary information, including the power-transfer relationships required for the computation in Subsections A can be gathered by the PE algorithm:

$$Rx_{th}^{PE} < Rx_{th} / K \qquad \textbf{(16)}$$

$$Rx_{th}^{PE} \leq Rx_{th}^{PCS} \qquad \textbf{(17)}$$

where Rx_{th}^{PE} is the receiver sensitivity threshold for PE packets, it should be set as the maximum of (16) and (17). The purpose of (16) and (17) is to ensure that the PE packets sent out by other interfering links or potentially interfering links within the *IntRange* can be received, so that the required information needed to execute steps 2 and 3 in per-iteration power adjustment can be obtained from the PE packets. The reader is referred to Appendix I for the formal proof that (16) and (17) can ensure that a node can gather the required power information for per-iteration power adjustment in our power adjustment algorithm.

C. Implementation of DAPC

We now discuss implementation issues with regard to the PE algorithm. According to (16) and (17), the receiver sensitivity for PE packets must be higher than that for regular DATA packets and at least that for PHY header. If each node transmits its PE and DATA packets at the same power, then we could transmit PE packets at the same rate as that of PHY header.

Consider IEEE 802.11b. The data rate of DATA is 11Mbps. The PHY header is transmitted at 1Mbps. Inequality (17) can be satisfied if we also transmit PE packets at 1 Mbps. In addition, to the extent that the receiver sensitivity can be improved by a factor of 11 (to maintain the same energy per bit for 1Mbps and 11Mbps), then (16) can also be satisfied. This is because $Rx_{th}^{PE} = Rx_{th}^{PCS} = Rx_{th} / 11 < Rx_{th} / K$ with K=10 (the typical 10dB SIR requirement).

The above argument is based on the same-energy-per-bit assumption. Since different coding schemes are used for 1Mbps and 11Mbps, this assumption may not apply strictly. NS-2 simulates what is found in a commercial product, such as Atheros 802.11 chips. In its default setting [8], *PCSRange* = 550m, while *TxRange* = 250m. So, *PCSRange* = 2.2**TxRange*. Assuming PE packets has the range as the PHY header, *PCSRange*, the implied receiver sensitivities are related by $Rx_{th}^{PE} / Rx_{th} = 1/2.2^{\alpha}$, where α is the path-loss exponent. Any $\alpha > 2.92$ guarantees that $Rx_{th}^{PE} / Rx_{th} < 1/K$ where K = 10. The default α value in NS-2 is 4. So, PE data rate of 1Mbps is also sufficient by this argument.

In the IEEE 802.11 standard, there are two commonly used modes for clear channel assessment (CCA). I) Energy Decision bases the CCA decision only on whether the energy detected is over a threshold. II) Carrier Sense bases the CCA decision purely upon whether an 802.11 signal is detected (i.e., successful detection of an 802.11 PHY header). The carrier sensing discussed in this paper assumes the support of mode II, and probably mode I, where the threshold in mode I is higher than that in mode II in general. According to mode II, since the medium is regarded as busy whenever the PHY headers from other links are decodable, PE packets can be decoded if they are transmitted with the same rate as the PHY headers.

One may notice that there are potential collisions of broadcast PE packets with other packets, including regular packets, other PE packets, or non-802.11 sources. Since broadcast packets have no ACK, each PE packet may need to be transmitted several times (e.g., three times in our assumption) to make sure it is received by all the intended receivers.

Note that the distributed DAPC is robust in that even if all the three PE packets were missed by an intended receiver node, the node will simply assume the "worst-case" in which it is assumed that the node whose PE packets have been missed continue to use the previous higher power.

D. Deadlock Problem in DAPC

In DAPC, every link adjusts its power while assuming the powers of neighboring links remain unchanged. In this case, they may run into a deadlock. An illustrating example is shown in Figure 5. In the figure, links 1 and 2 are of unit length. Suppose that all the nodes are currently using the same transmit powers. The nodes of links 1 and 2 do not interfere with each other according to inequalities (1) – (4), since they are separated by distance of $K^{1/\alpha}$ units, which is equal to the interference margin.

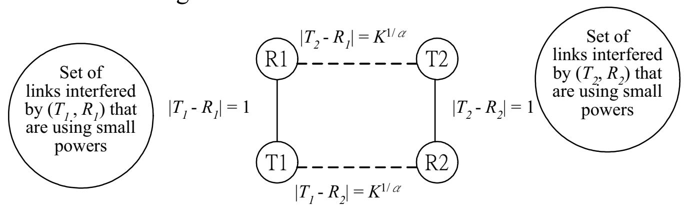

Figure 5. Illustration of the deadlock problem of DAPC.

However, if link 1 (link 2) adjusts its power down while link 2 (link 1) does not adjust its power, a new i-edge will be created from link 2 to link 1. Thus, according to DAPC, no power reductions will be allowed for links 1 and 2.

On the other hand, if both links 1 and 2 adjust their powers down by the same amount, i-edges will not be created between them since the SIR remains the same. Reducing powers as such may be desirable because it may reduce the interferences of links 1 and 2 to other nearby links, leading to elimination of i-edges from links 1 and 2 to them. DAPC cannot achieve this, and will be stuck in the suboptimal solution in which the powers of links 1 and 2 will remain high indefinitely. We refer to this as the *deadlock problem.*

Definition of Deadlock:
An algorithm is said to run into a deadlock if:
(1) no further power adjustment is possible according to the algorithm;
(2) however, one can identify a set of links whose powers can be further adjusted down simultaneously without creating new i-edges while maintaining link connectivity and HN-free property.

Note that part (2) of the above definition only requires that no new i-edges are created. In general, reducing powers may also eliminate some of the old i-edges, although this is not a requirement according to the definition. The idea is that we would like to use as small powers as possible.

To reduce the likelihood of deadlock (or more specifically, to ensure that when deadlocks occur, the power levels are already low), we may perform Uniformly-Scaled Power Control (USPC) [1], where we selects a *common* and *uniform* initial transmit power for all nodes that is sufficiently low before launching DAPC. Figure 7a shows the performance of DAPC and DAPC with pre-USPC. The reader is referred to Section V for the detailed simulation settings. For the case with pre-USPC, we set the initial transmit power so that the initial *TxRange* corresponds to half the diagonal of a square in the grid.

We see from the figure that DAPC with pre-USPC (DAPC-PU) can achieve a smaller number of attacking cases than DAPC alone. In particular, the performance of DAPC-PU is within 22% from the benchmark, which corresponds to the result of the minimum-transmit power approach, in which all nodes use just enough power to maintain its link connectivity. Note that the benchmark case is one in which there are the fewest numbers of tc- and rc-edges, but in which there may be excessive numbers of HN.

IV. PROGRESSIVE-UNIFORMLY-SCALED POWER CONTROL (PUSPC): DEADLOCK-FREE DESIGN

This section presents our second distributed adaptive power control algorithm, called *Progressive-Uniformly-Scaled Power Control (PUSPC)*, which is deadlock-free. In Subsection A, we present the details of the algorithm, followed by the proof of its deadlock-free property in Subsection B. Subsection C considers deadlock-free resolution for DAPC by applying the concept of PUSPC, and Subsection D presents an incremental power adaptation algorithm that modifies PUSPC for situations where the nodes are mobile and the network topology can change dynamically.

A. Algorithm of PUSPC

In PUSPC, we divide the links into *PowerControlSet* and *FinishedSet*. Initially, all links are in the *PowerControlSet* and they will start with the same initial power. They then reduce their powers by a common quantized size in each iteration and the algorithm is synchronized. As time progresses, some links will be placed in the *FinishedSet* and their powers will not be further adjusted while the links in *PowerControlSet* continue to reduce their powers in future iterations. At any one time, all links in *PowerControlSet* have the same uniform powers, while links in *FinishedSet* may have different powers.

```
// PUSPC executed by a node k in each iteration.
// Set the step size for power control and initial power level.
S = stepsize;
P_d = initial power level;
// Backtrack Algorithm
if (the link of node k receives a FinishedSet declaration from link l and finds that it has
  over reduced its power){
     raise transmit power of node k to an appropriate level such that no new i-edge is
     formed from link l;
     if (the link of node k is in PowerControlSet)
        move the link of node k to FinishedSet;
}
else if (link of node k in PowerControlSet){
   if (P_d <= S)
      move link of node k to FinishedSet;
   else {
      P_d = P_d – S;      // next power level
      // (i) make sure the link of the node is not disconnected
      if (the link of node k disconnected if its transmit power is reduced to P_d){
         move the link of node k to FinishedSet;
         break;
      }
      else{
         for (each link l whose PE packets can reach node k){
            // (ii) Make sure no new i-edge is formed from link l to the link of node k
            if (a new i-edge is formed from link l to the link of node k if its transmit
            power is reduced to P_d) {
                  move the link of node k to FinishedSet;
                  break;
            }
            // (iii) Make sure the PCSRange is enough to cover interfering nodes
            else if (there is an existing i-edge from link l to the link of node k, and the
              PHY header of node k cannot reach link l if its transmit power is reduced
              to P_d){
                  move the link of node k to FinishedSet;
                  break;
            }
         }
      }
      If (node k is not in FinishedSet)
         set transmit power of node k to P_d;
   }
}
```

Figure 6. Pseudo-code of PUSPC executed by a node *k*.

In each iteration, each node *k* whose link is in *PowerControlSet* can further reduce its power by the quantized size if three conditions below are satisfied:

(i) Its link will not be disconnected after power adjustment.

(ii) No new i-edge will be formed from links in *FinishedSet* to its links after power adjustment. Note that no *new* i-edge will be formed among links in *PowerControlSet* since their powers are the same and adjusted by the same amount – i.e., there is no change in SIR. In addition, no new tc- or rc-edges will be created by reducing power.

(iii) Its *PCSRange* is enough to cover interfering nodes after power adjustment. In this constraint, node *k* needs to check that the *PCSRange* is still sufficient to reach the nodes in interfering links.

Note that (i), (ii) and (iii) are similar to steps 1, 2 and 3 in Section III.A, except that for (ii), we assume the other links in *PowerControlSet* adjust their powers by the same amount in the same iteration; whereas in step 2, we assume the other links will use the powers that they used in the previous iteration. Essentially for PUSPC, N_{R1} and N_{T1} in (13) and (14) should include only nodes whose links are in *FinishedSet*.

In PUSPC, we can add one more bit in the PE packet called the "Set Index" to indicate whether a link is in *PowerControlSet* or *FinishedSet*, when a link goes into *FinishedSet* from *PowerControlSet*, it will declare to neighboring links by setting Set Index. Similar to DAPC, each node only needs to monitor the PE packets from neighboring nodes within its *IntRange.*

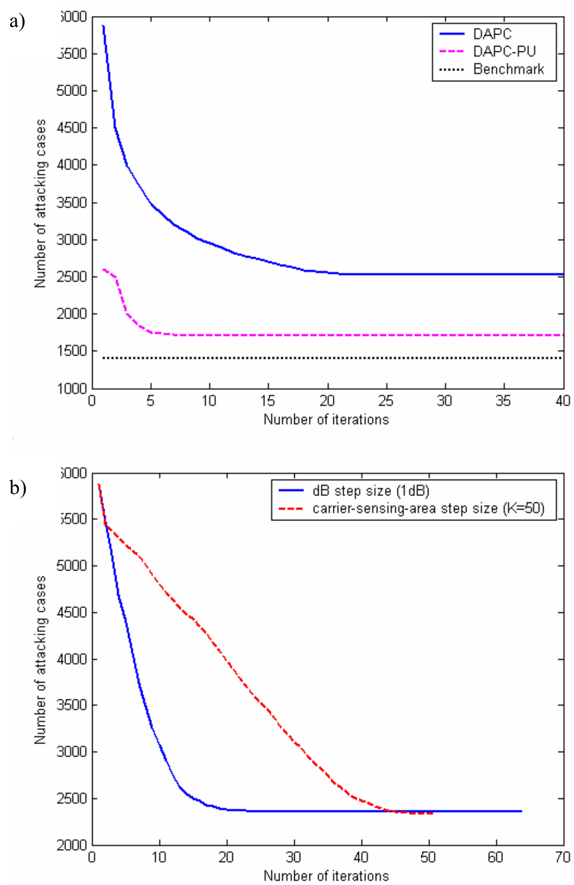

Figure 7. The no. of attacking cases against the no. of iterations of a) DAPC and DAPC-PU; and b) PUSPC with dB and carrier-sensing-area step size.

The quantized step size for power reduction is a crucial factor that affects the efficiency and accuracy of PUSPC. It is a trivial fact that links can reach a smaller power level with a smaller step size or more iterations, and a larger number of attacking cases can be reduced. In our simulations, we considered two definitions for step size: (i) dB step size: we reduce the power by a constant amount (in unit of dB) in each iteration. (ii) carrier-sensing-area step size: we reduce the power in such a way that the area of the circle with radius *PCSRange* shrinks by a constant amount in each iteration.

The intuition of shrinking the circle defined by the *PCSRange* by a constant amount in each step is to ensure that the number of nodes that we consider in each step (or covered by the *PCSRange*) decreases at a constant rate, since the average number of nodes in an area A is $\rho*A$, where ρ is the node density. The reader is referred to [10] for the details of the carrier-sensing step size.

The simulation results of PUSPC with the dB step size (with a step size of 1dB) and the carrier-sensing-area step size (with the number of steps, K = 50) are shown in Figure 7b. We can see that the case with dB step size reduces attacking cases in the network at a faster rate at the beginning, while with carrier-sensing-area step size almost reduces attacking cases linearly. Finally, both approaches end with similar number of attacking cases.

B. Deadlock-free Property of PUSPC

We now prove that PUSPC is deadlock-free. As the power of nodes in *PowerControlSet* is adjusted down in successive iterations, there comes an iteration when the power of a "critical" link cannot be adjusted further, and this critical link will then be placed in the *FinishedSet*. There are two possible reasons why the power of the critical link cannot be adjusted further:

(i) Reducing the power further may cause either the critical link to be disconnected, or may cause its carrier-sensing range to fail to cover an interfering link from *FinishedSet* for HN-free operation.

(ii) Reducing the power further may create new i-edges from some link in *FinishedSet* to the critical link.

Note that (i) is not a cause of deadlock, because the power of the critical link cannot be adjusted down if the link connectivity and HN-free requirements are to be preserved. (see definition of deadlock condition (2) in Section III.D). That leaves us to prove that (ii) will not cause deadlock either. Since we are using quantized step size here, we redefine part of the definition of deadlock (2) in Section III.D to "(2) however, one can identify a set of links whose powers can be further adjusted down by the quantized step size, S, simultaneously without creating new i-edges while maintaining link connectivity and HN-free property." With this modification of deadlock definition, we have the following proposition:

Proposition 1:
There is no deadlock in the solution produced by PUSPC.

Proof: Consider a link, say link 1, in *PowerControlSet*. Suppose that in the current iteration, link 1 is the "critical" link that would violate constraint (ii) if its power were reduced further, and that there would be a new i-edge formed from link 2 in *FinishedSet* to link 1. In PUSPC, Link 1 will be moved to *FinishedSet*, and the power adjustment will be the power level just above the critical power adjustment. We show that deadlock involving link 1 and other links in *FinishedSet* is not possible at the end of this iteration. By induction, after the last iteration when all links have been added to *FinishedSet*, there will be no deadlocks in the overall network.

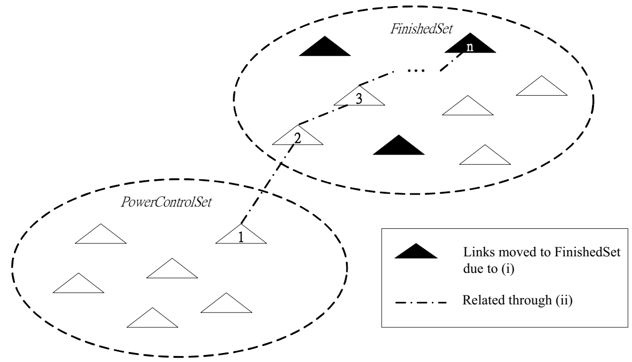

Figure 8. Graphical illustration of deadlock-free in PUSPC.

Suppose we assume on the contrary that there is deadlock involving link 1 and some other links in *FinishedSet*. That means it is possible to adjust the power of link 1 plus the power of some other links in *FinishedSet* without creating new i-edges. Say, the additional power adjustment is $\delta p > S$. If the power of link 1 is reduced by this amount, the power of link 2 should also be reduced by the same amount to maintain the same SIR so that no new i-edge is formed from link 2 to link 1. By the same token, if the power of link 2 is reduced by δp, the power of another link, say link 3, must also be adjusted since link 2 was a critical link in a previous iteration. Continuing this argument allows us to identify a set of links – link1, link 2, …, link n – whose powers must be adjusted down together, or else new i-edges may be formed. At some point, we will find a link, say link n, whose power cannot be adjusted down because of (i) rather than (ii) – in the "worst case", all links in *FinishedSet* are identified; however, the first link included in *FinishedSet* in the first iteration is always due to (i). A graphical illustration is shown in Figure 8, where the black triangle represents the link whose power cannot be adjusted because of (i). Certainly, it is not possible to adjust the power of link n by δp. We have thus shown that it is not possible to simultaneously adjust the powers of links 1, 2, ..., n simultaneously without creating an i-edge while maintaining link connectivity and HN-free property.

C. Deadlock Resolution for DAPC using PUSPC

As discussed in Section III, DAPC is not deadlock-free. Some nodes may reach a deadlock and remain at a high power level. As a result, some reducible tc- and rc-edges become irreducible. Although DAPC-PU discussed in Subsection III.D can achieve a smaller number of attacking cases, it is not deadlock-free. Also, it may be inconvenient to have to conduct the pre-USPC phase, since an implicit assumption is that we can find a "low" common initial power that all nodes can adopt.

For deadlock-free designs, an alternative to PUSPC in the previous subsection is to modify DAPC to eliminate deadlocks.

A two-step approach which consists of DAPC followed by PUSPC for deadlock resolution can be used. For the details of the algorithm, the reader is referred to [10].

Figure 9 shows the performance of DAPC with this Deadlock Resolution (DAPC-DR) and the original PUSPC in the previous subsection, both at a step size of 1dB. In the figure, the second portion of the curve for DAPC shows the performance of the deadlock resolution. Originally, DAPC stops with 2521 attacking cases, the deadlock resolution further pulls down the number of attacking cases to 2233. Although in this simulation setting, the number of attacking cases reduced by deadlock resolution is not large, it is still important to have it to guarantee the performance of DAPC. In other settings, there could be two links that hold on to large transmit powers because of deadlock. Such links with large powers will cause a large number of tc- and rc-edges in their neighborhood, resulting in unacceptable performance at portions of the network within their vicinities.

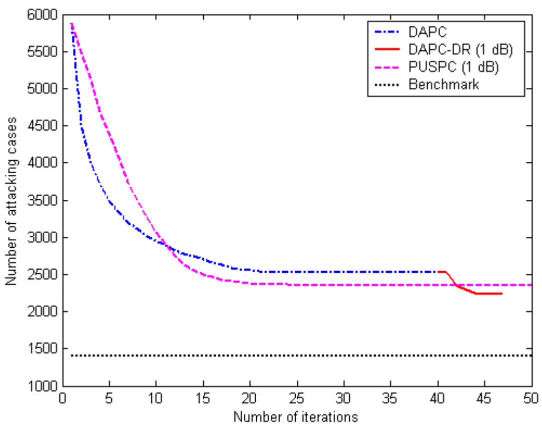

Figure 9. Simulation results of PUSPC and DAPC-DR.

D. Incremental Power Adaptation (IPA)

DAPC and PUSPC both assume that we reduce powers of links from a maximum common power level. In practice, one may be faced with situations in which the network topology changes incrementally. It will be interesting to study how to adapt the power incrementally rather than resetting the power level and adjust it from a maximum common power level. In this section, we introduce an Incremental Power Adaptation (IPA) algorithm that adjusts power levels in an incremental way. IPA modifies PUSPC to allow the power to be reduced as well as increased incrementally in response to node mobility. The IPA presented here strives to maintain a HN-free environment while adjusting power.

IPA consists of a number of synchronized iterations. In each iteration, the power level of a link can be raised, reduced by one step or remain unchanged, depending on the power levels of its neighboring links. And links exchange their power information through the PE Algorithm. We assume the step size used is in terms of dB, which means that the power level is either scaled up or down by a common factor upon a change in an iteration.

In each iteration in IPA, a link may decide to raise, reduce or maintain its power level based on the following considerations:

1. RAISE: It raises power by a step size when the current power level is not sufficient to maintain the connectivity of the link, or the associated *PCSRange* cannot reach certain interfering nodes.

2. REDUCE: It reduces power by a step size if the new lowered power level can still maintain the link connectivity, the associated *PCSRange* can still reach all interfering nodes, and new i-edges from other links will not be created, assuming other links use the same power levels at the end of the previous iteration (i.e., the power levels as gathered using the PE algorithm after the end of the previous iteration).

3. STATIONARY: If neither 1 (RAISE) nor 2 (REDUCE) is satisfied, the link will remain at its current power level.

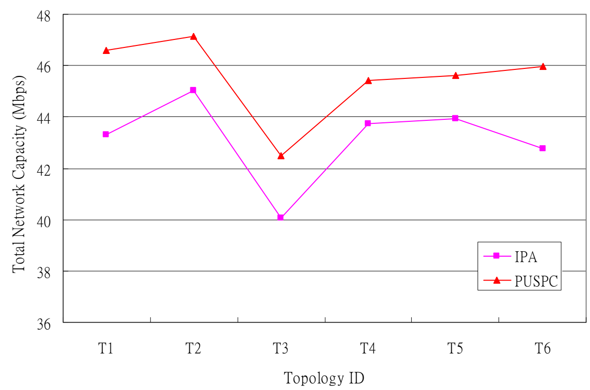

Figure 10. Overall network capacities of PUSPC and IPA in different topologies.

The major advantage of IPA compared with DAPC and PUSPC is that the algorithm is adaptable to topology changes, we do not need to reset the powers in a drastic manner for incremental movements of nodes. In practice, we can run IPA at synchronized time instances to update the power incrementally in a mobile network. Figure 10 shows the throughput performances of IPA and PUSPC in different topologies simulated in NS-2. In general, IPA can achieve about 95% of the network capacity of PUSPC. Due to the space limit here, the reader is referred to [10] for the detailed algorithm of IPA and more experimental results.

V. NUMERICAL PERFORMANCE RESULTS

In our simulations, we use a grid topology in a 1x1 km^2 domain. Each square in the grid contains an AP at the center. There are 25 APs, and 100 client stations placed randomly in the whole domain. Each client is connected to its closest AP. The initial transmit power of all nodes is 281.8mW or 232mW. We simulated the network in basic mode with the initial *PCSRange* $\geq$ 3.78 x *TxRange*, and Receiver Restart (RS) Mode is turned on. This setting guarantees that *the initial network is HN-free.*

The network capacities in Table I are obtained by simulations in NS-2. A UDP link with a rate of 6 Mbps is established from each client to its associated AP. Data rate of 11 Mbps, and packet size of 1460 bytes are assumed. Table I summarizes the overall simulation results of the ordinary non-power-controlled 802.11 (with a constant power level of 281.8mW or 232mW, where 232mW is the minimum transmit power for guaranteeing the HN-free property in the network), minimum-transmit-power approach, DAPC-DR and PUSPC (both with a step size of 1dB).

Table I. Comparison of DAPC-DR, PUSPC with the minimum-transmit-power approach and ordinary 802.11.

	802.11 with RS Mode (HN-free)	Min-pow	DAPC-DR (1dB)	PUSPC (1dB)
# attacking cases	5879	1406	2233	2335
Total Network Capacity (NS-2) (Mbps)	19.69	46.63	45.09	49.00
# HN-causing edges	0	386	0	0
Miss Ratio (%)	0	45.31	0	0
# EN-causing edges	4428	80	1178	977
False-alarm Ratio (%)	519.72	9.39	198.99	129.58

We can see from the table that although the minimum-transmit-power approach gives us the smallest number of attacking cases, it creates more HN instances in the network, which initially does not exist. Moreover, PUSPC can achieve higher total network capacity than the minimum-transmit-power approach with no HN being created.

Table I shows the results with saturated traffic. Lighter loads are used in Table II, in which the data rate of the UDP flow is varied from 1 Mbps to 4 Mbps. It can be seen that the results are similar to those in Table I. In general, DAPC-DR and PUSPC can achieve two times more capacity than the ordinary non-power-controlled 802.11 network while guaranteeing that no HN is created in the process, and have higher throughput than minimum-transmit power approach in most cases.

Table II. Total network capacities of DAPC-DR, PUSPC, minimum-transmit-power approach and ordinary 802.11 with different data rates of UDP flow.

Data rate of UDP flow	1 Mbps	2 Mbps	4 Mbps
Ordinary 802.11 (281.8mW) (Mbps)	22.51	21.34	20.75
Minimum-transmit power approach (Mbps)	41.92	43.05	43.87
DAPC-DR (Mbps)	41.28	46.23	45.93
PUSPC (Mbps)	41.21	45.67	47.38

Table III shows the total network capacity of the three cases when the density of nodes increases from two clients per AP (50 clients and 25 APs) to eight clients per AP (200 clients and 25 APs). We observe that the total throughput of the network with PUSPC can be maintained at more than two times that achieved by the ordinary non-power-controlled 802.11 network when the node density increases. The minimum-transmit power approach has better improvement when the node density is low. However, the improvement diminishes quickly when the node density increases, due to the higher degree of HN.

Table III. Total network capacity of PUSPC, minimum-transmit-power approach and ordinary 802.11 with different node densities in the network.

Clients : APs	2 :1	4 :1	8 : 1
Ordinary 802.11 (281.8mW) (Mbps)	22.74	19.69	15.75
Minimum-transmit power approach (Mbps)	51.21	46.63	26.64
PUSPC (Mbps)	48.48	49.00	39.90

Trade-off between EN and HN

We have so far focused on elimination of HN entirely in the network. The HN-free algorithms we have considered, however, are actually amenable to modifications that aim to decrease EN at the cost of some HN. Figure 11a shows the variation in network capacity with the trade-off between HN and EN of the network with the client-AP ratio = 4 : 1. The settings considered include 1) a hidden-node free network without power control at the constant power level of 281.8mW; 2) a hidden-node free network with PUSPC; 3) a range of networks with constraint (iii) of PUSPC relaxed to allow progressively increasing number of HN-causing edges; and 4) the minimum-transmit-power approach.

The relaxation in 3) above is achieved by means of disregarding the coverage requirement of *PCSRange*. More specifically, we allow inequality (15) to be violated for a maximum of d times for each link. Thus, we can tune the degree of HN in the network by tuning d. Each time (15) is violated, the # HN-causing edges increases while the # EN-causing edges may decrease. As d increases, the curve asymptotically approaches the case with minimum-transmit powers. As a reference, we also plotted the throughput of the minimum-transmit-power approach as the last point of the curve.

In order to have a quantitative comparison of fairness in different schemes, we employ the Jain's Fairness Index [11] to measure the fairness of the networks with different degrees of HN. We can map the plot in Figure 11a point-by-point to a Jain's Fairness Index versus total network capacity plot, as shown in Figure 11b.

To compare the performance based on the plot in Figure 11b, let us define a two-dimensional metric called *Effectiveness*. Let $\rho(S_i)$ and $J(S_i)$ denote the total throughput and Jain's Fairness Index of solution i respectively. The effectiveness of solution i is denoted by $E(S_i) = [\rho(S_i), J(S_i)]$. We say that $E(S_1) \succ E(S_2)$ if and only if (i) $[\rho(S_1) > \rho(S_2)$ and $J(S_1) > J(S_2)]$; or (ii) $[\rho(S_1) > \rho(S_2)$ and $J(S_1) = J(S_2)]$; or (iii) $[\rho(S_1) = \rho(S_2)$ and $J(S_1) > J(S_2)]$.

From Figures 11a and b, we observe that for the solid-line part of the curve the total network capacity increases while Jain's Fairness Index decreases, validating the tradeoff between throughput and fairness. The solid-line part corresponds to a Pareto efficiency frontier [12], where the throughput cannot be improved without sacrificing fairness. In this "trade-off" region, we cannot definitely say one solution is more effective than another. The design decision is pretty much an exercise in finding the right balance between throughput and fairness, the trade-off of which is caused by the trade-off of the degrees of EN and HN in the network.

With reference to Figures 11a and b again, note that there is a turning point beyond which further increasing HN, although can reduce EN, actually causes the network capacity to go down. This corresponds to the dotted-line part of the curve. A reason why the throughput drops in this region could be that there are too many hidden nodes, and that causes the carrier-sensing mechanism to fail to prevent a large number of collisions. In the extreme that the network operates without carrier sensing, we are essentially left with an Aloha network, whose throughput is well known to be quite a bit lower than a network with carrier sensing in an analysis in which spectrum spatial re-use is not considered.

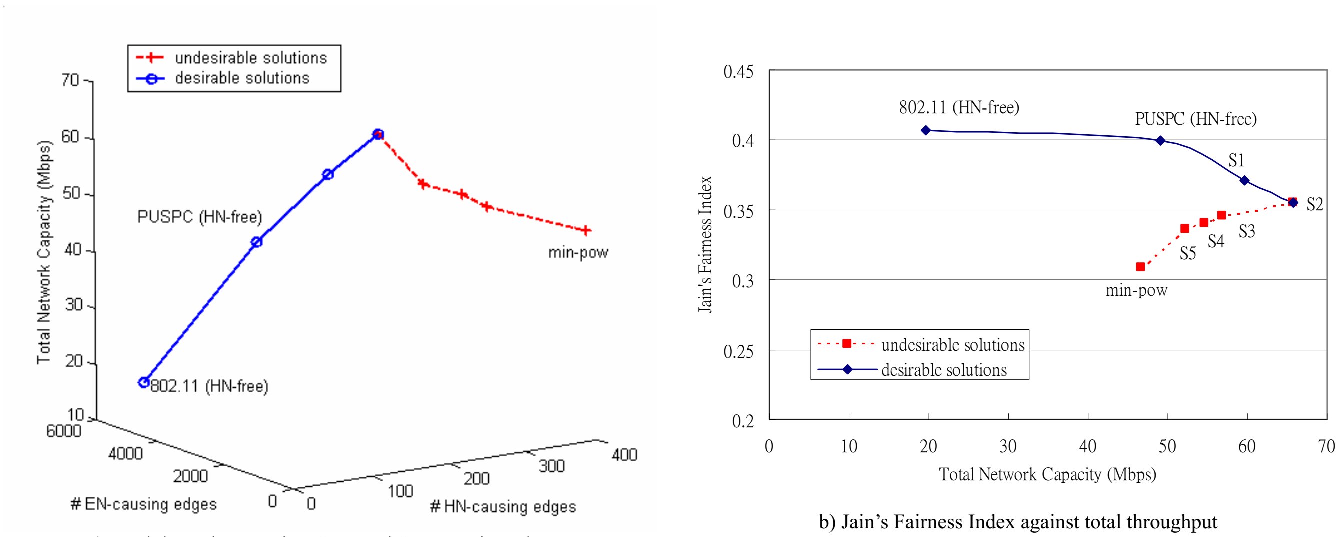

a) Total throughput against #HN and #EN-causing edges

b) Jain's Fairness Index against total throughput

Figure 11. Total network capacity and fairness with the trade-off between HN and EN from HN-free scenario to the minimum-transmit-power approach.

The dotted-line part of the curve is not Pareto efficient: effectiveness E decreases throughout this region, with $E(S_{min\text{-}pow})$ being the smallest. It is not desirable to operate in this region, because for each operating point p in this region, we can always find another operating point p' with $E(p') \succ E(p)$. For example, for the point S_3 in Figure 11b, both S_1 and S_2 are such that $E(S_1) \succ E(S_3)$ and $E(S_2) \succ E(S_3)$.

A simple example also serves to illustrate the relationship between throughput and fairness. Figure 12a shows the physical locations of three links, and Figures 12b, c and d show respectively the graph diagrams of the network with no power control, PUSPC and min-pow. The numerical results presented below are obtained from simulations.

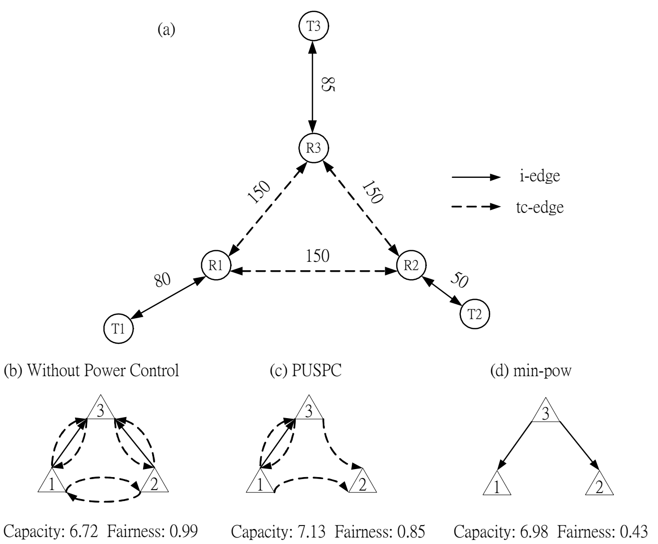

Figure 12. An example to illustrate the relationship between throughput and fairness.

In Figure 12b, every link can carrier-sense each other, so only one link is allowed to transmit at a time. The throughput of each link is about 2.2Mbps and the network is fair with Jain's Fairness Index = 0.99. PUSPC is used in Figure 12c, and therefore some i-edges and tc-edges have been eliminated compared with the situation in Figure 12b. In this case, link 2 can transmit simultaneously with link 1 or 3 given that link 2 starts the transmission before them (since there are only tc-edges from links 1 and 3 to 2, but not vice versa). It can be seen that the total throughput has been improved due to the spatial reuse, but there is degradation in fairness since link 2 may not be allowed to transmit when link 1 or 3 is already transmitting. The situation gets worse when we adopt min-pow in Figure 12d. Now the three links cannot carrier-sense each other, but there are interference relationships among them, which give rise to hidden nodes in the network. In this case, link 3 captures the channel and collisions happen at links 1 and 2. As a result, we observe that both the network capacity and fairness degrade with respect to Figure 12c, in which the Jain's Fairness Index is being halved.

VI. CONCLUSION

Transmit power control can be used to optimize spectral reuse in wireless networks. Most previous investigations [2] [3] adopt the minimum-transmit-power approach to reduce EN. HN and its associated problems remain. Our investigation has been an attempt to find better schemes than the minimum-transmit-power approach. Overall, the main contributions of this paper are three-fold:

1. We have shown by a counter example and simulation results that power control with minimum-transmit powers can create HN, which in turn causes a number of performance problems, including unfair bandwidth distributions in the network.
2. We have proposed and investigated two distributed adaptive power control algorithms: DAPC and PUSPC. When adjusting powers, these algorithms make sure that (i) no new interference relationships will be created beyond those already in existence; and (ii) no new HN will be created. These algorithms can achieve high spectral reuse

by reducing EN while avoiding HN entirely. Our simulation results show that DAPC and PUSPC on average can improve the network capacity of non-power-controlled 802.11 by more than two times. At the same time, PUSPC achieves both better fairness and higher network capacity than the minimum-transmit-power approach.

3. We have proposed using the concept of Pareto efficiency to compare the performance of different power control algorithms on the basis of network capacity and fairness. The HN-free algorithms in 2 above can be modified to allow a certain degree of HN to further reduce EN. By varying the degree of HN allowed in our algorithms, we can trade off network capacity against fairness, yielding a range of different operating points in which higher network capacity means lower fairness, and conversely, higher fairness means lower network capacity. However, when the degree of HN is too high, both network capacity and fairness deteriorate simultaneously, even with the reduced EN. This operating region, to which the minimum-transmit-power approach belongs, is *not* desirable.

APPENDIX I: Proof of the Correct Operation of PE Algorithm

> **Proposition 2:**
> If (16) and (17) are satisfied, the information needed for a node's *per-iteration power adjustment* can be gathered by itself and other nodes whose PE packets can reach it.

Proof: Lemma 1 in the following proves that the information required for step 1 of the per-iteration power adjustment algorithm can be obtained by a node. Lemmas 1 and 2 prove that information required for step 2 can be obtained. Lemma 3 proves that information required for step 3 can be obtained.

> **Lemma 1:**
> $G(T_1, R_1)$ can be determined by T_1 and R_1 if (16) is satisfied.

Proof of Lemma 1: By (16), the PE packets of R_1 can reach T_1. By examining the content of the PE packets from R_1, which contains $P(T_1, R_1)$, T_1 can determine $G(T_1, R_1) = P(T_1, R_1) / P_{T1}$. Similarly for R_1.

> **Lemma 2:**
> *Both* $P(n, T_1)$ $\forall n \in N_{T1}$ *and* $P(n, R_1)$ $\forall n \in N_{R1}$ can be determined by T_1 as well as R_1 if (16) is satisfied.

Proof of Lemma 2: We prove this lemma with respect to T_1. The proof for R_1 is similar. For step 2 of per-iteration power adjustment, T_1 needs to know $P(n, R_1)$ for all n that satisfies $P(n, R_1) > Rx_{th} / K$, Substituting (16) into the above, we have $P(n, R_1) > Rx_{th}^{PE}$.

This means that the PE packets of node n can reach and be decoded by R_1. By measuring the power of these PE packets, and by examining their content, which contains the source address of node n, R_1 can then derive the identity of n, and hence $P(n, R_1)$. According to the PE algorithm, this information is incorporated into the PE packets of R_1 and broadcasted. When T_1 receives the PE packets of R_1, T_1 obtains the information on $P(n, R_1)$. $P(n, R_1)$ is sufficient for T_1 to execute step 2 and $P(n, T_1)$ is not needed.

However, that $P(n, T_1)\ \forall n \in N_{T1}$ can also be obtained by T_1 follows from the same argument above that $P(n, R_1)$ $\forall n \in N_{R1}$ can be obtained by R_1.

> **Lemma 3:**
> $G(T_1, m)$ $\forall m \in M_{T1}$ can be determined by T_1 if (17) is satisfied.

Proof of Lemma 3: Consider a node $m \in M_{T1}$. If initially, the network is HN-free, then T_1 must be able to carrier-sense m. This means the PHY header of node m must be able to reach T_1 and decoded by it. So, $P(m, T_1) \geq Rx_{th}^{PCS} \geq Rx_{th}^{PE}$ by (17). Therefore, the PE packets from m can be received by T_1. By measuring the received power of the PE packets, and obtaining the identity of m and PS_m in the payload of the PE packets, $G(T_1, m)$ can be determined by T_1.

When we adjust the powers down, $\forall m \in M_{T1}$, step 3 in per-iteration power adjustment will ensure the *PCSRange* of node m continue to cover T_1 in the next iteration to maintain the HN-free property, which implies that the PE packets from node m will continue be able to reach T_1 in each and every successive iteration so long as $m \in M_{T1}$.

REFERENCES

[1] W. H. Ho, S. C. Liew, "Achieving Scalable Capacity in Wireless Networks with Adaptive Power Control," *the Fifth International IEEE Workshop on Wireless Local Networks (WLN)*, Nov 2005.

[2] V. Kawadia and P. R. Kumar, "Principles and Protocols for Power Control in Ad Hoc Networks," *IEEE Journal on Selected Areas in Communications*, pp. 76-88, vol.23, no. 5, Jan 2005.

[3] S. Agarwal, S. V. Krishnamurthy, R. H. Katz, S. K. Dao, "Distributed Power Control in Ad-hoc Wireless Networks," *Personal Indoor Mobile Radio Conference*, Oct 2001.

[4] J. P. Monks, V. Bharghavan, and Wen-mei Hwu, "A Power Controlled Multiple Access Protocol for Wireless Packet Networks," *IEEE INFOCOM*, 2001.

[5] L. B. Jiang and S. C. Liew, "Hidden-node Removal and Its Application in Cellular WiFi Networks," to appear in *IEEE Trans. on Vehicular Technology*. Shorter version appeared as "Removing Hidden Nodes in IEEE 802.11 Wireless Networks," in *IEEE Vehicular Technology Conference*, Sep 2005.

[6] P. C. Ng and S.C. Liew, "Throughput Analysis of IEEE 802.11 Multi-hop Ad hoc Networks," to appear in *IEEE/ACM Trans. on Networking*, 2007. Shorter version appeared as "Offered Load Control in IEEE802.11 Multi-hop Ad-hoc Networks," in the *1st IEEE International Conference on Mobile Ad-hoc and Sensor Systems (MASS)*, Oct 2004.

[7] E. Jung, N. Vaidya, "A Power Control MAC Protocol for Ad Hoc networks," *Mobicom*, 2002.

[8] "The Network Simulator – ns2", http://www.isi.edu/nsnam/ns.

[9] P. C. Ng, S. C. Liew, L. Jiang, "Achieving Scalable Performance in Large-Scale IEEE 802.11 Wireless Networks," *IEEE Wireless and Communications and Networking Conference*, Mar 2005.

[10] W. H. Ho, "Adaptive Power Control in Wireless Networks for Scalable and Fair Capacity Distributions," M. Phil. Thesis, The Chinese University of Hong Kong, May 2006.

[11] R. Jain, D. M. Chiu and W. Hawe, "A Quantitative Measure of Fairness and Discrimination For Resource Allocation in Shared Computer Systems," Technical Report TR-301, DEC Research Report, September, 1984.

[12] Milchtaich, I., "Network Topology and the Efficiency of Equilibrium," Department of Economics, Bar-Ilan University, Isreal, Working paper, First draft, Jun 2001.

[13] Anmol Sheth, Richard Han, "Adaptive Power Control and Selective Radio Activation for Low-Power Infrastructure-Mode 802.11 LANs," *ICDCSW'03*, May 2003.